CHAPTER 1:
Introduction

In This Chapter...

1.1 Instrument Overview

Wide Field and Planetary Camera 2 (WFPC2) is a two-dimensional imaging photometer which is located at the center of the Hubble Space Telescope (HST) focal plane and covers the spectral range between approximately 1150Å to 10500Å. It simultaneously images a 150″ x 150″ "L"-shaped region with a spatial sampling of 0.1″ per pixel, and a smaller 34″ x 34″ square field with 0.046″ per pixel. The total system quantum efficiency (WFPC2+HST) ranges from 5% to 13% at visual wavelengths, and drops to ~0.5% in the far UV. Detection of faint targets will be limited by either the sky background (for broad filters) or by noise in the read-out electronics (for narrow and UV filters) with an RMS equivalent to 5 detected photons. Bright targets can cause saturation (>53000 detected photons per pixel), but there are no related safety issues. The sections below give a more detailed overview.

1.1.1 Field-of-View

The WFPC2 field-of-view is divided into four cameras by a four-faceted pyramid mirror near the HST focal plane. Each of the four cameras contains an 800x800 pixel Loral CCD detector. Three cameras operate at an image scale of 0.1″ per pixel (F/12.9) and comprise the Wide Field Camera (WFC) with an "L" shaped field-of-view. The fourth camera operates at 0.046″ per pixel (F/28.3) and is referred to as the Planetary Camera (PC). There are thus four sets of relay optics and CCD sensors in WFPC2. The four cameras are called PC1, WF2, WF3, and WF4, and their fields-of-view are illustrated in Figure 1.1 (see also “CCD Position and Orientation on Sky” on page 159). Each image is a mosaic of three F/12.9 images and one F/28.3 image.

Figure 1.1: WFPC2 Field-of-View Projected on the Sky. The readout direction is marked with arrows near the start of the first row in each CCD. The X-Y coordinate directions are for POS-TARG commands. The position angle of V3 varies with pointing direction and observation epoch, and is given in the calibrated science header by keyword PA_V3.

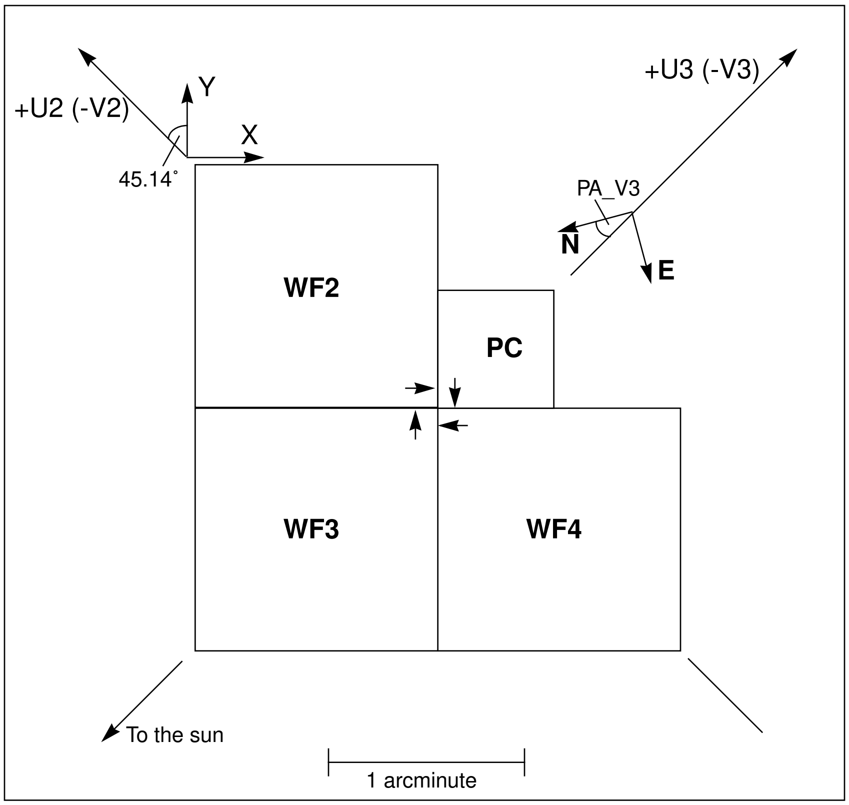

1.1.2 Spectral Filters

The WFPC2 contains 48 filters mounted in 12 wheels of the Selectable Optical Filter Assembly (SOFA). These include a set of broad band filters approximating Johnson-Cousins UBVRI, as well as a set of wide U, B, V, and R filters, and a set of medium bandwidth Strömgren *u, v*, *b*, and *y* filters.

Narrow band filters include those for emission lines of Ne V (3426Å), CN (~3900Å), [OIII] (4363Å and 5007Å), He II (4686Å), Hβ (4861Å), He I (5876Å), [OI] (6300Å), Hα (6563Å), [NII] (6583Å), [SII] (6716Å and 6731Å), and [SIII] (9531Å). The narrow-band filters are designed to have the same dimensionless bandpass profile. Center wavelengths and profiles are uniformly accurate over the filter clear apertures, and laboratory calibrations include profiles, blocking, and temperature shift coefficients.

There are also two narrow band “quad” filters, each containing four separate filters which image a limited field-of-view: the UV quad contains filters for observing redshifted [OII] emission and are centered at 3767Å, 3831Å, 3915Å, and 3993Å. The Methane quad contains filters at 5433Å, 6193Å, 7274Å, and 8929Å. Finally, there is a set of narrow band “linear ramp filters” (LRFs) which are continuously tunable from 3170Å to 9762Å; these provide a limited field-of-view with diameter ~10″.

At ultraviolet wavelengths there is a solar-blind Wood’s UV filter (1200-1900Å). The UV capability is also enhanced by control of UV absorbing molecular contamination, the capability to remove UV absorbing accumulations on cold CCD windows without disrupting the CCD quantum efficiencies and flat field calibrations, and an internal source of UV reference flat field images.

Finally, there is a set of four polarizers set at four different angles, which can be used in conjunction with other filters for polarimetric measurements. However, due to the relatively high instrumental polarization of WFPC2, they are probably suitable only for measurements on strongly polarized sources (>3% polarized).

1.1.3 Quantum Efficiency and Exposure Limits

The quantum efficiency (QE) of WFPC2+HST peaks at 13% in the red, and remains above 5% over the visible spectrum. The UV response extends to Lyman α wavelengths (QE~0.5%). Internal optics provide spherical aberration correction.

Exposures of bright targets are limited by saturation effects, which appear above ~53000 detected photons per pixel (for setting ATD-GAIN=15), and by the shortest exposure time which is 0.11 seconds. There are no instrument safety issues associated with bright targets. Detection of faint targets is limited by the sky background for broad band filters at visual wavelengths. For narrow band and ultraviolet filters, detections are limited by noise in the read-out amplifier (“read noise”), which contributes an RMS noise equivalent to ~5 detected photons per pixel.

1.1.4 CCD Detector Technology

The WFPC2 CCDs are thick, front-side illuminated devices made by Loral. They support multi-pinned phase (MPP) operation which eliminates quantum efficiency hysteresis. They have a Lumogen phosphor coating to give UV sensitivity. Details may be summarized as follows:

- **Read noise:** WFPC2 CCDs have ~5e^- RMS read noise which provides good faint object and UV imaging capabilities.

- **Dark noise:** Inverted phase operation yields low dark noise for WFPC2 CCDs. They are being operated at -88˚C and the median dark current is about 0.0045 e^{-} $pixel^{-1}$ s^{-1}.
- **Flat field:** WFPC2 CCDs have a uniform pixel-to-pixel response (<2% pixel-to-pixel non-uniformity) which facilitates accurate photometric calibration.
- **CTE:** Low level charge traps are present in the WFPC2 devices at the present operating temperature of -88˚C. On low background star fields, the traps result in a loss of about 4% of the signal when a star image is clocked down through all rows of the CCD. In the presence of background, the effect is reduced. For most applications, CTE is negligible or calibratable and pre-flash exposures are not required. This avoids the increase in background noise, and the decrease in operational efficiency that results from a preflash.
- **Gain switch:** Two CCD gains are available with WFPC2, a 7 e^{-} DN^{-1} channel which saturates at about 27000 e^{-} (4096 DN with a bias of about 300 DN) and a 14 e^{-} DN^{-1} channel which saturates at about 53000 e^{-}. The Loral devices have a full well capacity of ~90,000 e^{-} and are linear up to 4096 DN in both channels.
- **DQE:** The peak CCD DQE in the optical is 40% at 7000Å. In the UV (1100-4000Å) the DQE is determined by the phosphorescent Lumogen coating, and is 10 - 15%.
- **Image Purge:** The residual image resulting from a 100x (or more) full-well over-exposure is well below the read noise within 30 minutes. No CCD image purge is needed after observations of very bright objects. The Loral devices bleed almost exclusively along the columns.
- **Quantization:** The systematic Analog-to-Digital converter errors have been largely eliminated, contributing to a lower effective read noise.
- **QEH:** Quantum Efficiency Hysteresis (QEH) is not a significant problem in the Loral CCDs because they are frontside illuminated and use MPP operation. The absence of any significant QEH means that the devices do not need to be UV-flooded and the chips can be warmed monthly for decontamination purposes without needing to maintain a UV-flood.
- **Detector MTF:** The Loral devices do suffer from low level detector MTF perhaps caused by scattering in the frontside electrode structure. The effect is to blur images and decrease the limiting magnitude by about 0.5 magnitudes.

1.1.5 UV Imaging

WFPC2 had a design goal of 1% photometric stability at 1470Å over a month. This requires a contamination collection rate of less than 47 ng cm^{-2} $month^{-1}$ on the cold CCD window. Hence, the following features were designed into WFPC2 in an effort to reduce contaminants:

1. Venting and baffling, particularly of the electronics, were redesigned to isolate the optical cavity.
2. There was an extensive component selection and bake-out program, and specialized cleaning procedures.
3. Molecular absorbers (Zeolite) were incorporated.

The CCDs were initially operated at -77˚C after launch, which was a compromise between being as warm as possible for contamination reasons, while being sufficiently cold for an adequate dark rate. However, at this temperature significant photometric errors were introduced by low-level traps in the CCDs. This problem with the charge transfer efficiency of the CCDs has been reduced since 23 April 1994 by operating the CCDs at -88˚C, but this leads to significantly higher contamination rates than hoped for. On-orbit measurements indicate that there is now a decrease in throughput at a repeatable rate of ~30% per month at 1700Å, and moreover, that monthly decontamination procedures are able to remove the contaminants completely and recover this loss.

1.1.6 Aberration Correction and Optical Alignment

WFPC2 contains internal corrections for the spherical aberration of the HST primary mirror. These corrections are made by highly aspheric surfaces figured onto the Cassegrain relay secondary mirror inside each of the four cameras. Complete correction of the aberration depends on a precise alignment between the OTA pupil and these relay mirrors.

Mechanisms inside WFPC2 allow optical alignment on-orbit. The 47˚ pick-off mirror has two-axis tilt capabilities provided by stepper motors and flexure linkages, to compensate for uncertainties in our knowledge of HST's latch positions (i.e., instrument tilt with respect to the HST optical axis). These latch uncertainties would be insignificant in an unaberrated telescope, but must be compensated for in a corrective optical system. In addition, three of the four fold mirrors, internal to the WFPC2 optical bench, have limited two-axis tilt motions provided by electrostrictive ceramic actuators and invar flexure mountings. Fold mirrors for the PC1, WF3, and WF4 cameras are articulated, while the WF2 fold mirror has a fixed invar mounting. A combination of the pick-off mirror and actuated fold mirror (AFMs) has allowed us to correct for pupil image misalignments in all four cameras. Since the initial alignment, stability has been such that mirror adjustments have not been necessary. The mechanisms are not available for GO commanding.

1.2 Which Instrument to Use: WFPC2, FOC, NICMOS, or STIS?

In this section we compare briefly the performance of HST instruments with imaging capability in the UV to near-IR spectral range. As of this writing, both WFPC2 and FOC have capabilities in this area. Two new instruments, the Near-Infrared Camera and Multi-Object Spectrograph (NICMOS) and the Space Telescope Imaging Spectrograph (STIS) should be installed in HST during the second service mission in Early 1997. Important *imaging* parameters for all instruments are summarized in Table 1.1 below.

Table 1.1: Comparison of WFPC2, FOC, NICMOS, and STIS Instrumental Imaging Parameters.

Parameter	WFPC2	FOC[a]	NICMOS	STIS
Wavelength range	1150Å - 11,000Å	1150Å - 6500Å	8000Å - 25,000Å	FUV-MAMA: 1150Å - 1700Å NUV-MAMA: 1700Å - 3100Å CCD: 2000Å - 11,000Å
Detector	Si CCDs	Image Intensifier + EBS TV tube	HgCdTe CCDs	CCD, MAMAs
Image Format	4 x 800 x 800	128 x 128 up to 1024 x 512[b]	3 x 256 x 256	1024 x 1024
Field-of-view and pixel size	150″ x 150″ @ 0.1″ pix^{-1} 34″ x 34″ @ 0.046″ pix^{-1} [c]	up to 7″ x 7″ @ 0.014″ pix^{-1}	1: 11″ x 11″ @ 0.043″ pix^{-1} 2: 19″ x 19″ @ 0.075″ pix^{-1} 3: 51″ x 51″ @ 0.2″ pix^{-1}	MAMAs: 25″ x 25″ @ 0.024″ pix^{-1} CCD: 28″ x 50″ @ 0.05″ pix^{-1} [d]
Read noise	5 e^-	0	30 e^-	MAMAs: 0 e^- CCD: 4e^-
Dark current	0.004 $e^- s^{-1}$	0.0007 $e^- s^{-1}$	<0.1 $e^- s^{-1}$	MAMAs: <0.0001 $e^- s^{-1}$ CCD: 0.004 $e^- s^{-1}$
Saturation	53,000 e^-	2 count $s^{-1}pix^{-1}$	200,000 e^-	MAMAs: 100 count $s^{-1}pix^{-1}$ CCD: 170,000 e^-

a. Parameters given for only F/96 mode. F/48 mode is similar but pixels are twice as large.
b. 1024 x 512 mode uses 0.014″ x 0.028″ pixels to cover 14″ x 14″.
c. "L"-shaped field-of-view using 3 CCDs with 0.1″ pixels, and one CCD with 0.046″ pixels.
d. Field-of-view is 50″ x 50″ if no filter is used, and 12″ x 12″ for some neutral density filters.

1.2.1 Comparison of WFPC2 and FOC

Advantages of each instrument may be summarized as follows.

WFPC2 advantages are:

- Wider field-of-view, 150″ x 150″ vs. 7″ x 7″ or less.
- Higher throughput at λ>4500Å.

- Better flat field accuracy: WFPC2 accuracy of ~1% vs. few % for FOC. WFPC2 has no bright target safety issues, and can give useful data on faint targets near very bright objects. FOC can be damaged by bright objects.
- Better short-term geometric stability: FOC is impacted by geometric changes during turn-on and as a function of orbit position.

FOC advantages are:

- Higher throughput at λ<4500Å.
- Less impacted by far-UV contaminants.
- PSF sampling: FOC offers 0.014″ pixels vs. 0.0455″ on WFPC2.

The choice of instrument will be largely based on wavelength, required field-of-view, and need for good PSF sampling at short wavelengths. We note also that the FOC polarization data should be easier to calibrate, since there are fewer large-angle reflections than WFPC2, and since all polarization angles are available at all positions in the field-of-view.

Table 1.2: Comparison of WFPC2 and FOC Detective Efficiencies.

Instrument	Filter	Mean Wave-length (Å)	Bandpass FWHM (Å)[a]	Peak QE[b]
WFPC2	F122M	1420	100	0.12%
FOC	F140W	1370	298	0.25%
WFPC2	F255W	2586	393	0.45%
FOC	F220W	2280	480	1.2%
WFPC2	F336W	3342	500	2.9%
FOC	F342W	3410	702	5.4%
WFPC2	F439W	4300	700	3.4%
FOC	F430W	3940	832	4.7%
WFPC2	F547M	5476	660	10.6%
FOC	F550M	5460	188	0.83%

a. Note that definition of FWHM is different from “effective width” elsewhere herein.
b. Includes instrument and OTA.

1.2.2 Comparison of WFPC2 and NICMOS

Both WFPC2 and NICMOS are capable of imaging at wavelengths between ~8000Å and ~11,000Å. At longer wavelengths NICMOS must be used; at shorter wavelengths either WFPC2, FOC, or STIS must be used. Table 1.3 below compares the detective efficiency of WFPC2 and NICMOS in the wavelength region where both instruments are viable. Count rates for a V=20 star of spectral class A0 are given for all filters at common wavelengths; the signal-to-noise (S/N) is also given for a 1 hour exposure of this same star. For bright continuum sources WFPC2 and NICMOS offer similar efficiency over the spectral range from 8800Å to 10,500Å; the choice of instrument will likely depend on other factors such as field size and details of the passband shape. However, for very faint sources, the lower read noise of WFPC2 ($5e^-$ for WFPC2 vs. $30e^-$ for NICMOS) should prove advantageous.

Both instruments have a polarimetry capability, but the WFPC2 polarizers are not viable above 8000Å; above this wavelength NICMOS must be used for polarimetry.

Table 1.3: Comparison of WFPC2 and NICMOS Count Rates for V=20 A0 Star.

Instrument	Filter	Mean Wavelength (Å)	Effective Width (Å)	Count Rate ($e^{-} s^{-1}$)	SNR in 1 hour[a]
WFPC2	F785LP	9366	2095	14	215
	F791W	8006	1304	30	314
	F814W	8269	1758	33	333
	F850LP	9703	1670	7.1	150
	FQCH4N (Quad D)	8929	64	0.47	34, 29[b]
	F953N	9546	52	0.21	19, 15[b]
	F1042M	10,443	611	0.20	18, 15[b]
	LRF[c]	8000 9000 9762	105 113 126	1.5 0.64 0.23	66 40 20
NICMOS	F090M[d]	8970	1885	2.0	90
	F095N[d]	9536	88	0.14	12
	F097N[d]	9715	94	0.18	16
	F108N[d]	10,816	94	0.17	15
	F110W (Camera 1)	11,022	5920	6.6	160
	F110W (Camera 2)	11,035	5915	14	260
	F110W (Camera 3)	11,035	5915	26	350

a. WFPC2 SNR assuming two 1800s exposures for cosmic ray removal. NICMOS SNR for central pixel of PSF.
b. Values given for WFC (0.10″ pixels) and PC (0.046″ pixels).
c. LRF filter is continuously tunable from 3710Å to 9762Å. LRF field-of-view is 10″x10″.
d. These NICMOS filters are available only on Camera 1 which has 11″ x 11″ field-of-view.

1.2.3 Comparison of WFPC2 and STIS

Both WFPC2 and STIS are capable of imaging over the same wavelength ranges between ~1150Å and ~11000Å. At much longer wavelengths NICMOS must be used.

Advantages of each instrument may be summarized as follows.

WFPC2 advantages are:

- Wider field-of-view, 150″ x 150″ vs. 50″ x 50″ or less.
- Greater selection of filters, including polarizers.
- Flat field accuracy: WFPC2 is likely to have better flat fielding, since geometry is highly stable. STIS filters are near focal plane and geometry may be unstable due to Mode Selection Mechanism non-repeatability.
- Field uniformity: STIS focus varies across field in image modes.
- Bright Targets: WFPC2 has no bright target safety issues, and can give useful data on faint targets near very bright objects. STIS MAMAs can be damaged by bright objects.

STIS advantages are:

- Much higher UV throughput.
- True solar blind imaging in UV due to MAMA detectors. WFPC2 CCDs are very sensitive to filter red-leak.
- PSF sampling: STIS offers 0.024″ pixels vs. 0.0455″ on WFPC2.
- High time resolution is possible (τ ~125μs) with the MAMA detectors. Also the STIS CCD may be cycled on ~10s timescale using a sub-array.

In general, WFPC2 has a much greater selection of filters and wider field-of-view than STIS, but STIS will have greater detective efficiency in the UV and for its long-pass and unfiltered modes. Table 1.2 below compares the detective efficiency for WFPC2 and STIS filters with similar bandpasses. For UV imaging STIS will be greatly superior due to higher throughput and insensitivity to filter red-leak; only if some detail of a WFPC2 filter bandpass were needed, would it be a viable choice.

For both [OII] 3727Å and [OIII] 5007Å imaging STIS has much higher QE and will be preferred, unless the larger WFPC2 field-of-view is an important factor. The WFPC2 [OIII] filter is wider than its STIS counter-part, which may also be useful for redshifted lines. For broad-band imaging the unfiltered and 5500Å long-pass modes of STIS again will have higher efficiency than WFPC2, though with reduced field-of-view.

Table 1.4: Comparison of WFPC2 and STIS Detective Efficiencies.

Instrument	Filter	Mean Wave-length (Å)	Bandpass FWHM (Å)[a]	Peak QE[b]
WFPC2	F122M	1420	100	0.12%
STIS	F25LYA	1216	85	4.0%
WFPC2	F160BW	1492	500	0.065%
STIS	FUV-MAMA	~1300	300	4.5%
WFPC2	F255W	2586	393	0.45%
STIS	NUV-MAMA	~2400	1300	3.4%
WFPC2	F375N	3738	42	0.8%
STIS	F28X50OII	3740	80	5%
WFPC2	F502N	5013	37	5%
STIS	F28X50OIII	5007	5	15%
WFPC2	F606W	5935	2200	13%
STIS	F28X50LP	~7300[c]	2600	21%
STIS	F50CCD	~5800	4500	22%

a. Note that definition of FWHM is different from “effective width” elsewhere herein.
b. Includes instrument and OTA.
c. 5500Å long pass filter.

1.3 History of WFPC2

The original Wide Field and Planetary Camera (WF/PC-1) served as the prototype for WFPC2. In many respects the two instruments are very similar. Both were designed to operate from 1150Å to 11000Å, both use 800x800 CCD detectors, and both provide spatial samplings of ~0.045″ and ~0.1″ per pixel. The development and construction of WF/PC-1 was led by Prof. J. A. Westphal, Principal Investigator (PI) of the California Institute of Technology. The instrument was built at the Jet Propulsion Laboratory (JPL) and was launched aboard HST in April 1990. It obtained scientific data until it was replaced by WFPC2 during the first service mission in December 1993.

Because of its important role in the overall HST mission, NASA decided to build a second Wide Field and Planetary Camera (WFPC2) as a backup clone of

WF/PC-1 even before HST was launched. WFPC2 was already in the early stages of construction at JPL when HST was launched. After the discovery of spherical aberration in the HST primary mirror, it was quickly realized that a modification of the WFPC2 internal optics could correct the aberration and restore most of the originally expected imaging performance. As a result, development of WFPC2 was accelerated. Dr. J. T. Trauger of JPL is the project PI for WFPC2 and led the Investigation Definition Team (IDT).

The WFPC2 completed system level thermal vacuum (SLTV) testing at JPL in April and May 1993. Between June and November there were payload compatibility checks at Goddard Space Flight Center (GSFC), and payload integration at Kennedy Space Center (KSC). WF/PC-1 was replaced by WFPC2 during the first Servicing Mission in December 1993. WFPC2 was shown to meet most of its engineering and scientific performance requirements by testing conducted during the three month Servicing Mission Observatory Verification (SMOV) period following the servicing mission. The General Observer community has had access to WFPC2 since the start of Cycle 4 in January 1994.

WFPC2 accurately corrects the HST spherical aberration, is a scientifically capable camera configured for reliable operation in space without maintenance, and is an instrument which can be calibrated and maintained without excessive operational overhead. It incorporates evolutionary improvements in photometric imaging capabilities. The CCD sensors, signal chain electronics, filter set, UV performance, internal calibrations, and operational efficiency have all been improved through new technologies and lessons learned from WF/PC-1 operations and the HST experience since launch.

WFPC2 SMOV requirements were developed by the IDT, GSFC, and the STScI to include: verification of the baseline instrument performance; an optical adjustment by focusing and aligning to minimize coma; the estimation of residual wavefront errors from the analysis of star images; a photometric calibration with a core set of filters (including both visible and UV wavelengths); and the evaluation of photometric accuracy and stability over the full field with the core filter set. The results of these studies are documented in Holtzman, et al., 1995a and 1995b, and are summarized in this Handbook.

Despite these successes, the first years of scientific operation of WFPC2 have revealed a number of relatively minor instrumental defects that were not expected from the pre-launch testing. These include a low-level charge transfer inefficiency, a higher than expected level of scattered light around bright objects, and variable and lower than expected ultraviolet (UV) efficiency. In addition, we have come to understand the instrument more fully -- particularly in terms of its overall photometric performance, geometric distortion, scale and alignments, hot pixels, and CCD traps. All of this new information is described here.

1.4 The Previous vs. Current Generation: WF/PC-1 vs. WFPC2

For historical reasons, it is useful to offer comparisons between the current WFPC2, and its predecessor WF/PC-1, which was returned to Earth in December 1993.

- **Field format:** WF/PC-1 contained 8 cameras and CCDs, each CCD having 800 x 800 pixels. Four were used in the Planetary Camera mode (0.043″ pixels), and four were used in the Wide Field Camera mode (0.10″ pixels). The two pixel formats were selected by rotating the pyramid mirror by 45°. WFPC2 budget and schedule constraints forced a reduction from 8 to 4 camera channels in August 1991. WFPC2 contains only 4 CCDs; the pyramid mirror is fixed and the 4 cameras are physically located in the bays occupied by the WF/PC-1 WFC.
- **Aberration correction:** WF/PC-1 contained no correction for spherical aberration of the OTA primary mirror. Only about 15% of light from a stellar target fell into the core of the PSF (diameter ~0.1″). WFPC2 incorporates corrective figures on the Cassegrain secondary mirrors inside the relay cameras, and as a result places ~60% of the light from a star inside a diameter of 0.1″. Precise alignment of the OTA pupil on these mirrors is required to attain full correction of the spherical aberration. Hence the pick-off mirror (POM) is steerable in WFPC2, and three of the fold mirrors contain tip-tilt actuators.
- **CCD Technology:** Many properties of WF/PC-1 and WFPC2 CCDs are compared in Table 4.1 on page 65. Many differences derive from the fact that the WF/PC-1 CCDs were thinned, backside illuminated devices whereas the WFPC2 CCDs are thick, frontside illuminated devices. WF/PC-1 CCDs were thinned and backside illuminated. The active silicon layer was a free-standing membrane somewhat less than 10µm thick, with photons impinging directly on the silicon layer, without attenuation in the polysilicon gate structure built on the other ('front') side of the device.
- **Quantum Efficiency Hysteresis (QEH):** The WF/PC-1 CCD's required a UV flood procedure and continuous cold temperatures to avoid QEH and hence non-linearity. A UV flood was performed early in the WF/PC-1 mission, but could not be repeated due to problems with the HST magnetometers. This in turn limited the temperature range allowable during decontaminations, since high temperatures would remove the UV flood, which in turn severely limited UV science capabilities. Some QE instability was also seen, particularly in the B band, due to changes in the UV flood. WFPC2 CCDs support multi-pinned phase (MPP) operation which eliminates quantum efficiency hysteresis.
- **Charge Transfer Efficiency:** WF/PC-1 devices suffered from significant charge transfer efficiency (CTE) errors at image intensities below ~200 electrons per pixel. This was overcome by preflashing virtually all science images. WFPC2 devices have very little CTE error, and hence no preflash is

used. Low-level charge traps are present in the WFPC2 devices, and result in a loss of about 4% of the signal when a star image is clocked down through all rows of the CCD. In the presence of background, the effect is reduced. For most applications, CTE is negligible or calibratable and pre-flash exposures are not required.

- **Detector MTF:** The WFPC2 Loral devices do suffer from poorer CCD detector MTF than the WF/PC-1 CCDs, perhaps caused by scattering in the frontside electrode structure. The effect is to blur images and decrease the limiting magnitude by about 0.5 magnitudes.
- **Flat field quality:** WF/PC-1 CCDs were chemically thinned devices and therefore varied in thickness across the field-of-view causing large features in the flat fields. WFPC2 CCDs are un-thinned and the intrinsic response is uniform to ~3% across the field.
- **DQE:** The WFPC2 CCDs have intrinsically lower QE than WF/PC-1 CCDs above 4800Å, which is due to attenuation by frontside electrode structures.
- **Gain switch:** WF/PC-1 had only a single analog-to-digital converter gain setting of 8 e^{-} DN^{-1} which saturated at about 30,000e^{-}. Two gains are available with WFPC2: a 7 e^{-} DN^{-1} channel which gives reasonable sampling of the 5e^{-} read noise, and which saturates at about 27,000e^{-}, and a 14 e^{-} DN^{-1} channel which saturates at about 53,000e^{-} and extends the useful dynamic range.
- **Quantization:** The systematic analog-to-digital converter errors that were present in the low order bits on WF/PC-1 have been largely eliminated, contributing to a lower effective read noise in WFPC2.
- **Calibration Channel:** WF/PC-1 contained a solar UV flood channel which was physically in the location of the present WFPC2 calibration channel. This transmitted solar UV light into the camera to provide a UV flood capability.
- **Entry Port:** The WF/PC-1 camera was sealed by an afocal MgF_2 window immediately behind the shutter. The WFPC2 entry port is open.
- **Chronographic Capability:** WF/PC-1 contained a low reflectance spot on the pyramid (known as the Baum spot) which could be used to occult bright objects. This has been eliminated from WFPC2, since the spherical aberration severely reduces its utility.
- **Contamination Control:** Since launch, WF/PC-1 suffered from the accumulation of molecular contaminants on the cold (-87˚C) CCD windows. This molecular accumulation resulted in the loss of FUV (1150-2000Å) throughput and attenuation at wavelengths as long as 5000Å. Another feature of the contamination was the “measles” — multiple isolated patches of low volatility contamination on the CCD window. Measles were present even after decontamination cycles, when most of the accumulated molecular contaminants were boiled off by warming the CCDs. In addition to preventing UV imaging, these molecular contamination layers scattered light and seriously impacted the calibration of the instrument. WFPC2 has far

less contamination than WF/PC-1 owing to pre-launch cleaning and bake-out procedures, careful design of venting paths to protect the optical bench area, and inclusion of Zeolite molecular absorbers in the design. There is now a decrease in throughput of about 30% per month at 1700Å, but monthly decontamination procedures completely remove this material. This throughput drop is also highly predictable and can be calibrated out during photometric analyses.

1.5 Organization of this Handbook

A description of the instrument is contained in Chapter 2. The filter set is described in Chapter 3. CCD performance is discussed in Chapter 4. A description of the Point Spread Function is given in Chapter 5. The details necessary to estimate exposure times are described in Chapter 6. A summary of observation strategies is given in Chapter 7. Data products and standard calibration methods, and calibration plans are summarized in Chapter 8. A complete list of references is given in Chapter 9.

This document summarizes the performance of the WFPC2 as known in April 1996 after two years of on-orbit calibration. Observers are encouraged to contact the STScI Help Desk, the WFPC2 WWW pages (see section 1.7 "WFPC2 Handbook on the WWW" below), and STScI Instrument Scientists for the latest information.

1.6 What's New in Version 4.0

Major revisions since Version 3.0 may be summarized as follows:

- Comparisons to FOC, STIS, and NICMOS.
- Observation Strategies: A new chapter (Ch. 7) has been added specifically to assist observers in preparing Phase II proposals.
- Exposure Time Estimation: Ch. 6 has been largely re-written. Signal-to-noise ratio equations for Poisson-limited, background-limited, and generalized cases are now included for point sources (both with PSF fitting and aperture photometry) and extended sources. The WWW on-line Exposure Time Calculator program is briefly described. A new Appendix gives representative SNR values for various exposures of stellar, power law, and emission line sources.
- CCD Performance: Material on dark current and CTE (charge transfer efficiency) has been updated.
- Calibration: Material on UV throughput, dark current calibration, flat fielding, and impact of focus variations on photometry has been updated. Cycle 6 calibration proposals are described.

- Other changes include addition of an index and an acronym list.

1.7 WFPC2 Handbook on the WWW

This Handbook will appear on the WFPC2 WWW pages accessible at:

`http://www.stsci.edu/ftp/instrument_news/WFPC2/top_wfpc2.html`

and will be updated as new information becomes available.

1.8 The Help Desk at STScI

STScI maintains a Help Desk whose staff quickly provide answers to any HST-related topic, including questions about WFPC2 and the Cycle 7 proposal process. The Help Desk staff has access to all of the resources available at the Institute. They maintain a database of frequently asked questions and answers, so that many questions can be answered immediately. The Help Desk staff can also provide copies of STScI documentation, in either hardcopy or electronic form, including Instrument Science Reports and Instrument Handbooks.

Questions sent to the Help Desk during normal business hours are usually answered within one hour. Questions received outside normal business hours will be answered within the first two hours of the next business day. Usually, the Help Desk staff will reply with the answer to a question, but occasionally they will need more time to investigate the answer. In these cases, they will reply with an estimate of the time needed to reply with the full answer.

We ask that you please send *all* initial inquiries to the Help Desk. If your question requires a WFPC2 Instrument Scientist to answer it, the Help Desk staff will put a WFPC2 Instrument Scientist in contact with you. By sending your request to the Help Desk, you are guaranteed that someone will provide a timely response.

To contact the Help Desk at STScI:

- **Send e-mail:** `help@stsci.edu`
- **Phone:** 1-410-338-1082

The Space Telescope European Coordinating Facility (ST-ECF) also maintains a Help Desk. European users should generally contact the ST-ECF for help; all other users should contact STScI.

To contact the ST-ECF Help Desk in Europe:

- **Send e-mail:** `stdesk@eso.org`.

1.9 Further Information

The material contained in this Handbook is derived from ground tests and design information obtained by the IDT and the engineering team at JPL, and from on-orbit measurements. Other sources of information are listed below. A complete list of references appears on page 197.

- *HST Phase II Proposal Instructions*, (Version 8.0, 15 December 1995).[1]
- *HST Data Handbook*, (Version 2.0, December 1996).[1]
- *Calibrating Hubble Space Telescope: Post Service Mission* (1995).[1]
- *STSDAS Calibration Guide*, (November 1991).[1]
- *The Reduction of WF/PC Camera Images*, Lauer, T., P.A.S.P. 101, 445 (1989).
- *The Imaging Performance of the Hubble Space Telescope*, Burrows, C. J., et. al., Ap. J. Lett., 369, L21 (1991).
- Interface Control Document (ICD) 19, "PODPS to STSDAS"
- Interface Control Document (ICD) 47, "PODPS to CDBS"
- *The Wide Field/Planetary Camera in The Space Telescope Observatory*, J. Westphal and the WF/PC-1 IDT, IAU 18th General Assembly, Patras, NASA CP-2244 (1982).
- *The WFPC2 Science Calibration Report*, Pre-launch Version 1.2, J. Trauger, editor, (1993). [IDT calibration report]
- *White Paper for WFPC2 Far-Ultraviolet Science*, J. T. Clarke and the WFPC2 IDT (1992)[1].
- *The Performance and Calibration of WFPC2 on the Hubble Space Telescope*, Holtzman, J., et al., P.A.S.P., 107, 156 (1995).
- *The Photometric Performance and Calibration of WFPC2*, Holtzman, J., et al., P.A.S.P., 107, 1065 (1995).
- The Institute's WFPC2 World Wide Web page at address: `http://www.stsci.edu/ftp/instrument_news/WFPC2/wfpc2_top.html`
- The Institute's WFPC2 Space Telescope Analysis Newsletter (STAN), which is distributed monthly via e-mail, and provides notification of any changes in the instrument or its calibration. To subscribe, send e-mail to `help@stsci.edu`.

1. These documents may be requested by e-mail from `help@stsci.edu`.